J. Mod. Power Syst. Clean Energy (2019) 7(4):705–715
https://doi.org/10.1007/s40565-019-0555-0

A three-stage approach for resilience-constrained scheduling of networked microgrids

Saeed TEIMOURZADEH[1], Osman Bulent TOR[1], Mahmut Erkut CEBECI[1], Adela BARA[2], Simona Vasilica OPREA[2]

Abstract This paper deals with optimal scheduling of networked microgrids (NMGs) considering resilience constraints. The proposed scheme attempts to mitigate the damaging impacts of electricity interruptions by effectively exploiting NMG capabilities. A three-stage framework is proposed. In Stage 1, the optimal scheduling of NMGs is studied through determining the power transaction between the NMGs and upstream network, the output power of distributed energy resources (DERs), commitment status of conventional DERs as well as demand-side reserves. In Stage 2, the decisions made at Stage 1 are realized considering uncertainties pertaining to renewable generation, market price, power consumption of loads, and unintentional islanding of NMGs from the upstream network and resynchronization. Stage 3 deals with uncertainties of unintentional islanding of each MG from the rest of islanded NMGs and resynchronization. The problem is formulated as a mixed-integer linear programming problem and its effectiveness is assured by simulation studies.

Keywords Networked microgrid (NMG), Distributed energy resource (DER), Power system resilience, Point estimate method

CrossCheck date: 18 April 2019

Received: 16 November 2018 / Accepted: 18 April 2019 / Published online: 2 July 2019

✉ Saeed TEIMOURZADEH
saeed@epra.com.tr

Osman Bulent TOR
osman.tor@epra.com.tr

Mahmut Erkut CEBECI
erkut.cebeci@epra.com.tr

Adela BARA
bara.adela@ie.ase.ro

Simona Vasilica OPREA
simona.oprea@csie.ase.ro

[1] Engineering, Procurement, Research and Analysis (EPRA) Electric Energy Co., Ankara, Turkey

[2] Department of Economic Informatics and Cybernetics, Faculty of Cybernetics, Statistics and Economic Informatics, Bucharest University of Economic Studies (BUES), Bucharest, Romania

1 Introduction

Recent weather-related events such as severe thunderstorms, hurricanes, and blizzards have significantly affected the normal operation of power systems around the globe [1]. Under extreme circumstances, the power systems represent vulnerable and non-resilient behavior which leads to major load interruptions and blackouts [2]. Due to the climate changes, the frequency and severity of catastrophic events might increase in the near future, implying the significance of power system resilience against such incidents [3].

Resilience notion is described from various perspectives which can be clustered into two categories [3–6]. One is the adaption standpoint defining the resilience attribute as the ability of power system to tolerate some unexpected events by accommodating to the dominant condition. The other one is restoration standpoint where the resilience is defined as the ability of the power system to retrieve its normal operation subsequent to certain extreme events. Despite the differences in viewpoints, low probability and high impact of the investigated events are highlighted. This paper considers adaption standpoint to study the resilience.

Among the available solutions in the literature, the deployment of distributed systems such as microgrids (MGs) is effective to enhance power system resilience and retain electricity procurement [7, 8]. Through the seamless islanded operation capability, MGs can ride through the outages until the restoration of disrupted main grid. In the islanded mode, the critical loads such as hospitals, police stations, security buildings, and data centers can be supplied by the on-site distributed energy resources (DERs) and managed by local controllers. Reference [9] offers a new framework for taking advantages of MG capabilities to ride through the islanding condition and improve resilience metrics. In [10], a robust optimization-based model is presented which seeks for minimum load interruption in islanding operation mode. It is demonstrated that the consideration of resilience issue in MGs scheduling is an effective measure to reduce the amount of load interruption in case of islanding. Reference [11] proposes a techno-economic model to utilize MG capabilities and surviving the critical loads during the islanding condition. The detailed analyses are performed to investigate the impact of demand-side reserve cost on MG operation. In addition, alterations in market prices, DER production, and load variations in real-time operation are taken into account. In [12], the coordination of demand-side reserves and storage units connected to an MG is considered with the objective of retraining MG stability while operating in islanding mode.

Extreme events and resultant MGs islanding are random phenomena which challenge the effectiveness of scheduling schemes in improving resilience metrics. To cope with this issue, stochastic programing-based approaches are presented in [13, 14]. Here, the expected costs(ECs) pertaining to the uncertain decision, e.g. renewable generation and islanding event are added to the cost of MG scheduling and the total cost is minimized subject to the suite of technical constraints. The other scheme to neutralize the effect of uncertainties is proactive scheduling [15–17]. In proactive methods, the MG follows its normal schedule right before receiving islanding alert which declares that the islanding might happen due to the approaching extreme event (e.g. windstorm). In this situation, the MG operator adapts proper precautions to minimize the effects of the approaching event. In proactive methods, the uncertainty of MG islanding is only considered.

The number of distributed elements is one of the most significant factors which affects resilience indexes [1]. Due to uneven propagation of damages, the level of resilience enhancement can be intensified as the number of distributed elements increases. This can be realized by increasing the number of local DERs or connecting adjacent MGs and establishing networked MGs (NMGs). In this paper, resiliency-oriented scheduling of NMGs is studied through a three-stage framework. The first stage deals with optimal scheduling of NMGs in normal operation conditions where the power transaction between the NMGs and upstream network, output power of DERs, commitment status of conventional DERs, and demand-side reserves are determined. In the second and third stages, the effect of prevailing uncertainties on real-time operation of NMGs is investigated. The second stage highlights unintentional islanding of NMGs from the upstream network and resynchronization; whereas, the third stage deals with uncertainties pertaining to the unintentional islanding of each MG from the rest of islanded NMGs. The problem is formulated as a mixed-integer linear programming problem and its effectiveness is assured by simulation studies.

2 Proposed methodology

2.1 Overview

The proposed three-stage approach is as follows.

Stage 1: Determining power transaction between NMGs and upstream network, DER output power, commitment status of conventional DERs, and demand-side reserves.

Stage 2: Realizing the decisions made at *Stage 1*; determining trasactions between each MG and the rest of NMGs; considering uncertainties and pertaining the to renewable generation, market price, power consumption of loads, and unintentional islanding of NMGs form the upstream network and resynchronization.

Stage 3: Realizing the decisions made at *Stage 1* and *Stage 2*; considering the uncertainties pertaining to unintentional islanding of MG from the rest of NMGs and resynchronization.

The outline of the proposed three-stage approach for resilience-constrained scheduling of NMGs is depicted in Fig. 1. Ω^{S2} and Ω^{S3} are the set of scenarios at *Stage 2* and *Stage 3*.

In Fig. 1, the objective is to attain a resilient NMGs which is capable of handling both normal operation and contingency-based uncertainties. This approach lies within stochastic programming-based [18] model as shown in Fig. 1, where the distribution of input data is first approximated by a collection of plausible sets (scenario generation). Then, the problem is formulated in a stochastic optimization fashion which implicitly weights (with the probabilities of occurrence) the solution of each input set with the aim of attaining a single solution. The achieved solution is adequately pre-positioned with respect to all the sets of input data, but not to any one of them particularly, which is an approach to the stochastic solution of the problem at hand.

In this framework, the scheduling of a resilient NMGs is modeled in *Stage 1* (Root) before the realization of any uncertainty. The decisions made in this stage include power

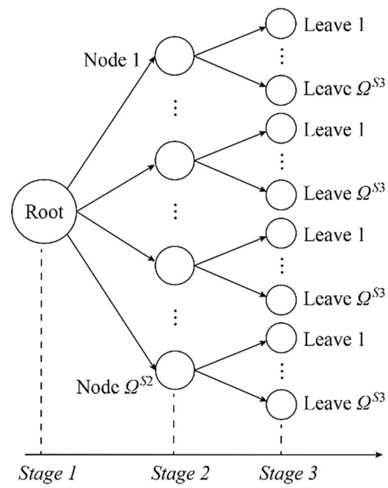

Fig. 1 Framework of the proposed three-stage approach

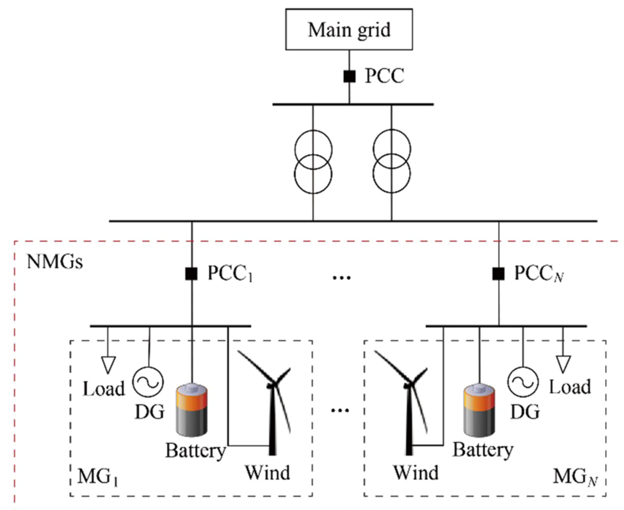

Fig. 2 An overview of a typical NMGs

transaction between the NMGs and upstream network, DERs output power, commitment status of conventional DERs, and demand-side reserves which are independent from the upcoming scenarios. Afterwards, proper sets of scenarios are generated for simulating the transitions between *Stage 1* and *Stage 2*. To generate the scenarios, the random variables are first described via probability distribution function (PDF). Then the PDFs are fed into the point estimate procedure [19] to calculate the possible scenarios. The random variables for *Stage 2* are wind generation, market price, power consumption of loads, and unintentional islanding of NMGs from the upstream network and resynchronization. Based on the realization of each scenario at *Stage 2*, unintentional islanding of each MG from the rest of NMGs and its resynchronization might happen which is also a random variable. These uncertainties are tackled by determining proper scenarios corresponding to transitions between *Stage 2* and *Stage 3*.

The detailed formulations of the proposed three-stage model are given in the following.

2.2 Objective function

Figure 2 depicts an overview of a typical NMGs, which is considered for problem formulation. The objective function for the proposed framework is to minimize total operation cost of NMGs. The total operation cost includes the cost of decisions made at *Stage 1* (before the realization of uncertainties) and EC of *Stage 2* and *Stage 3* which is influenced by the occurrence of specific scenarios. Mathematically, the objective function is:

$$\min \quad OF = \sum_{t \in I_T} \left(C_t^{S1} + EC_t^{S2,S3} \right) \tag{1}$$

$$\begin{aligned} C_t^{S1} &= \lambda_t^{M,Buy} P_{t,N\mu}^{S1,Buy} - \lambda_t^{M,Sell} P_{t,N\mu}^{S1,Sell} \\ &+ \sum_{\mu \in I_\mu} \left(\lambda_{t\mu}^{L,U} LR_{t\mu}^{S1,U} + \lambda_{t\mu}^{L,D} LR_{t\mu}^{S1,D} + \lambda_{t\mu}^{DG} P_{t\mu}^{S1,DG} \right) \end{aligned} \tag{2}$$

$$EC_t^{S2,S3} = \sum_{\omega \in \Omega^{S2}} \pi_\omega \left(A_{t\omega} + \sum_{\varphi \in \Omega^{S3}} \pi_\varphi B_{t\varphi} \right) \tag{3}$$

$$\begin{aligned} A_{t\omega} = &\lambda_{t\omega}^{RT,Buy+} \Delta P_{t\omega,N\mu}^{S2,Buy+} - \lambda_{t\omega}^{RT,Buy-} \Delta P_{t\omega,N\mu}^{S2,Buy-} \\ &+ \lambda_{t\omega}^{RT,Sell-} \Delta P_{t\omega,N\mu}^{S2,Sell-} - \lambda_{t\omega}^{RT,Sell+} \Delta P_{t\omega,N\mu}^{S2,Sell+} \\ &+ \sum_{\mu \in I_\mu} \left(\lambda_{t\mu}^{SU} u_{t\omega\mu}^{S2,SU} + \lambda_{t\mu}^{DG} P_{t\omega\mu}^{S2,DG} \right) \\ &+ \sum_{\mu \in I_\mu} \lambda_{t\mu}^{Dep} \left(LR_{t\omega\mu}^{S2,U} - LR_{t\omega\mu}^{S2,D} \right) \end{aligned} \tag{4}$$

$$\begin{aligned} B_{t\omega} = &\sum_{\mu \in I_\mu} \left(\lambda_{t\mu}^{SU} u_{t\varphi\mu}^{S3,SU} + \lambda_{t\mu}^{DG} P_{t\varphi\mu}^{S3,DG} \right) \\ &+ \sum_{\mu \in I_\mu} \lambda_{t\mu}^{Shed} P_{t\varphi\mu}^{S3,Shed} \end{aligned} \tag{5}$$

where t, I_T are index and set of time; μ, I_μ are index and set of MGs; ω is index realized at *Stage 2*; φ, Ω^{S3} are index realized at *Stage 2*; *Buy, Sell* are superscript for buying from and selling to market; *Dep, SU* are superscript for deployment and start-up; *Shed* is superscript for load shedding; *S*1, *S*2, *S*3 are superscript for *Stage 1*, *Stage 2*, and *Stage 3*; *DG, L* are symbol for conventional distributed generation (DG) and load; *M* is symbol for market-related quantities; N_μ is symbol for NMGs; *RT* is symbol for real-time quantities; *U, D* are up and down variations; +, − are positive and negative deviations; *LR* is demand-side reserve; *P* is active power; *u* is commitment status; λ is price per megawatt; and π is the probability of scenario.

In (1) and (2), C_t^{S1} represents the total cost for normal operation of the NMGs which encompasses the cost of power exchange between the NMGs and upstream network, the cost of scheduling demand-side reserves, and the cost of deploying conventional distributed generations within the NMGs. The EC of uncertain stages, i.e., *Stage 2* and *Stage 3*, are calculated by (3)-(5). For each scenario associated with *Stage 2*, $A_{t\omega}$ models the cost of realizing the decisions made at *Stage 1* which is the cost of adjusting power exchange, demand-side reserve deployment cost, starting up and using DGs within the NMGs. Likewise, for each scenario associated with *Stage 3*, $B_{t\omega}$ describes the start-up and production costs of DGs as well as possible load shedding cost within an MG which is islanded from the rest of NMGs. The devised objective function is minimized subject to the following constraints.

2.3 Constraints of Stage 1

The suite of constraints for *Stage 1* decisions is:

$$P_{t,N\mu}^{S1,Buy} - P_{t,N\mu}^{S1,Sell} + \sum_{\mu\in I_\mu} P_{t\mu}^{S1,Net} = 0 \tag{6}$$

$$P_{t\mu}^{S1,Net} = P_{t\mu}^{S1,DG} + P_{t\mu}^{S1,Wind} - P_{t\mu}^{S1,Bat+} + P_{t\mu}^{S1,Bat-} - P_{t\mu}^{S1,L} \tag{7}$$

$$0 \le P_{t,N\mu}^{S1,Buy} \le \alpha_{t,N\mu}^{S1} P_{t,N\mu}^{Buy,\max} \tag{8}$$

$$0 \le P_{t,N\mu}^{S1,Sell} \le \left(1-\alpha_{t,N\mu}^{S1}\right) P_{t,N\mu}^{Sell,\max} \tag{9}$$

$$\alpha_{t\mu}^{S1,DG} P_{\mu}^{DG,\min} \le P_{t\mu}^{S1,DG} \le \alpha_{t\mu}^{S1,DG} P_{\mu}^{DG,\max} \tag{10}$$

$$P_{\mu}^{Wind,\min} \le P_{\mu}^{S1,Wind} \le P_{\mu}^{Wind,\max} \tag{11}$$

$$P_{t\mu}^{L,\min} \le P_{t\mu}^{S1,L} \le P_{t\mu}^{L,\max} \tag{12}$$

$$0 \le LR_{t\mu}^{S1,U} \le LR_{t\mu}^{U,\max} \tag{13}$$

$$0 \le LR_{t\mu}^{S1,D} \le LR_{t\mu}^{D,\max} \tag{14}$$

$$0 \le P_{t\mu}^{S1,Bat+} \le \alpha_{t\mu}^{S1,Bat} P_{\mu}^{Bat+,\max} \tag{15}$$

$$0 \le P_{t\mu}^{S1,\,Bat-} \le \eta_{\mu}^{Bat}\left(1-\alpha_{t\mu}^{S1,\,Bat}\right) P_{\mu}^{Bat-,\,\max} \tag{16}$$

$$SoC_{t\mu}^{S1,Bat} = SoC_{(t-1)\mu}^{S1,Bat} + \frac{\eta_{\mu}^{Bat}\Delta t}{E_{\mu}^{Bat,\max}}\left(P_{(t-1)\mu}^{S1,Bat+} - (\eta_{\mu}^{Bat})^{-2} P_{(t-1)\mu}^{S1,Bat-}\right) \tag{17}$$

$$SoC_{\mu}^{Bat,\min} \le SoC_{t\mu}^{S1,Bat} \le SoC_{\mu}^{Bat,\max} \tag{18}$$

where *Bat* is the symbol for storage; *Wind* is the symbol for wind generation; min, max are symbols for lower and upper limits, respectively; *E* is energy capacity for storage unit; *SoC* is state of charge for storage unit; and *H* is conversion efficiency coefficient for storage unit.

In (6), the power balance between the NMGs and the upstream network is evaluated. Here, $P_{t\mu}^{S1,Net}$ represents the power transaction of each MG with the rest of NMGs and the upstream network. As can be seen from Fig. 2, each MG is represented as an equivalent conventional DG, wind generation, storage system, and load which can play the role of net load or generation for the rest of system. Equations (8)-(12) ensure that the decision variables in this stage, i.e. power to be traded with the upstream network, DG and wind generations, load consumption, demand-side reserves, and storage charged or discharged power, lie within associated upper and lower limits. In (8) and (9), the binary variable $\alpha_{t,N\mu}^{S1}$ is used to avoid enabling both selling and buying options at the same time. Likewise, the binary variable $\alpha_{t\mu}^{S1,Bat}$ averts simultaneous enabling of charging or discharging options associated with the storage unit in each MG. Finally, the binary variable $\alpha_{t\mu}^{S1,DG}$ identifies the commitment status of DG at *Stage 1*. The state of charge (SoC) for the storage system is calculated in (17) which is also required to reside within a predefined boundaries (18).

Once the decisions at *Stage 1* are made, optimal operation of NMGs within the permissible range is assured. However, such decisions are not subjected to the uncertainties. The uncertainties are taken into account by the proper constraints tailored at *Stages 2* and *3*.

2.4 Constraints of Stage 2

In this stage, the real-time operation of NMGs is studied by realizing the decisions made at *Stage 1*. Note that all variables in this stage depend on the envisioned scenario. The first step is to check the power balance which is:

$$P_{t\omega,N\mu}^{S2,Buy} - P_{t\omega,N\mu}^{S2,Sell} + \sum_{\mu\in I_\mu} P_{t\omega\mu}^{S2,Net} = 0 \tag{19}$$

In (19), the first two terms express the power trade of NMGs with the upstream network, i.e., $P_{t\omega,N\mu}^{S2,Buy}$ and $P_{t\omega,N\mu}^{S2,Sell}$, which are calculated as:

$$P_{t\omega,N\mu}^{S2,Buy} = P_{t,N\mu}^{S1,Buy} + \Delta P_{t\omega,N\mu}^{S2,Buy+} - \Delta P_{t\omega,N\mu}^{S2,Buy-} \tag{20}$$

$$P_{t\omega,N\mu}^{S2,Sell} = P_{t,N\mu}^{S1,Sell} + \Delta P_{t\omega,N\mu}^{S2,Sell+} - \Delta P_{t\omega,N\mu}^{S2,Sell-} \tag{21}$$

Equations (20) and (21) state that the realized power transaction between the NMGs might deviate from the scheduled value, $P_{t,N\mu}^{S1,Buy}$ and $P_{t\omega,N\mu}^{S2,Sell}$, which can be adjusted by positive and negative deviation variables, that is $\Delta P_{t\omega,N\mu}^{S2\,Buy+}$, $\Delta P_{t\omega,N\mu}^{S2\,Buy-}$, $\Delta P_{t\omega,N\mu}^{S2,Sell+}$, and $\Delta P_{t\omega,N\mu}^{S2,Sell-}$. The set of constraints involve in the process of calculating (20) and (21) is:

$$0 \le P_{t\omega,N\mu}^{S2,Buy} \le \tau_{t\omega}\alpha_{t\omega,N\mu}^{S2} P_{t,N\mu}^{Buy,\max} \tag{22}$$

$$0 \leq P^{S2,Sell}_{t\omega,N\mu} \leq \tau_{t\omega}\left(1-\alpha^{S2}_{t\omega,N\mu}\right)P^{Sell,\max}_{t,N\mu} \quad (23)$$

$$0 \leq \Delta P^{S2,Buy+}_{t\omega,N\mu} \leq BM(1-\beta^{Buy}_{t\omega}) \quad (24)$$

$$0 \leq \Delta P^{S2,Buy-}_{t\omega,N\mu} \leq BM\beta^{Buy}_{t\omega} \quad (25)$$

$$0 \leq \Delta P^{S2,Sell+}_{t\omega,N\mu} \leq BM(1-\beta^{Sell}_{t\omega}) \quad (26)$$

$$0 \leq \Delta P^{S2,Sell-}_{t\omega,N\mu} \leq BM\beta^{Sell}_{t\omega} \quad (27)$$

The objective behind (22) and (23) is similar to that of (8) and (9) where for each scenario, the binary variable $\alpha^{S2}_{t\omega,N\mu}$ determines the direction of power flow between the NMGs and the upstream network. Here, the binary parameter $\tau_{t\omega}$ is also used as an indicator for islanding and resynchronization events:

$$\tau_{t\omega} = \begin{cases} 0 & T^{Island}_{\omega,N\mu} \leq t \leq T^{Rsynch}_{\omega,N\mu} \\ 1 & \text{Otherwise} \end{cases} \quad (28)$$

where $T^{Island}_{\omega,N\mu}$ and $T^{Rsynch}_{\omega,N\mu}$ are islanding and resynchronization time for the NMGs. Hence during islanded operation, the power transaction between the NMGs and upstream network is fixed on zero and the DERs within the islanded NMGs supplying the loads.

Constraints (24)-(27) determine the boundaries of deviations for the variables in (20) and (21). The binary variables $\beta^{Buy}_{t\omega}$ and $\beta^{Sell}_{t\omega}$ identify the direction of deviations pertaining to buy the power from the market and sell to the market scenarios, respectively. In (24)-(27), BM is a relatively large positive scalar.

The last term in (19), $P^{S2,Net}_{t\omega\mu}$ is the real-time value of active power consumed or generated by each MG, which can be calculated as:

$$P^{S2,Net}_{t\omega\mu} = P^{S2,DG}_{t\omega\mu} + P^{S2,Wind}_{t\omega\mu} - P^{S2,Bat+}_{t\omega\mu} + P^{S2,Bat-}_{t\omega\mu} - P^{S2,L}_{t\omega\mu} \quad (29)$$

In (29), the DG generation should be within the predefined limits if already committed, i.e., $\alpha^{S2,DG}_{t\omega\mu} = 1$:

$$\alpha^{S2,DG}_{t\omega\mu}P^{DG,\min}_{\mu} \leq P^{S2,DG}_{t\omega\mu} \leq \alpha^{S2,DG}_{t\omega\mu}P^{DG,\max}_{\mu} \quad (30)$$

Otherwise, if starting a DG unit is necessary, associated start-up cost is calculated as (31) and reflected in the objective function using the linking binary variable as $u^{S2,SU}_{t\omega\mu}$:

$$\begin{cases} u^{S2,SU}_{t\omega\mu} \geq \alpha^{S2,DG}_{t\omega\mu} - \alpha^{S2,DG}_{(t-1)\omega\mu} \\ u^{S2,SU}_{t\omega\mu} \geq 0 \end{cases} \quad (31)$$

The wind generation $P^{S2,Wind}_{t\omega\mu}$ in (29) is derived from the scenarios under study; whereas, the active power taken from or stored in the storage $P^{S2,Bat-}_{t\omega\mu}$ and $P^{S2,Bat+}_{t\omega\mu}$ should satisfy the following constraints:

$$0 \leq P^{S2,Bat+}_{t\omega\mu} \leq \alpha^{S2,Bat}_{t\omega\mu}P^{Bat+,\max}_{\mu} \quad (32)$$

$$0 \leq P^{S2,Bat-}_{t\omega\mu} \leq \eta^{Bat}_{\mu}\left(1-\alpha^{S2,Bat}_{t\omega\mu}\right)P^{Bat-,\max}_{\mu} \quad (33)$$

$$SoC^{S2,Bat}_{t\omega\mu} = SoC^{S2,Bat}_{(t-1)\omega\mu} + \frac{\eta^{Bat}_{\mu}\Delta t}{E^{Bat,\max}_{\mu}}\left(P^{S2,Bat+}_{(t-1)\omega\mu} - (\eta^{Bat}_{\mu})^{-2}P^{S2,Bat-}_{(t-1)\omega\mu}\right) \quad (34)$$

$$SoC^{Bat,\min}_{\mu} \leq SoC^{S2,Bat}_{t\omega\mu} \leq SoC^{Bat,\max}_{\mu} \quad (35)$$

The last term $P^{S2,L}_{t\omega\mu}$ in (29) is the real-time value of the load at each MG which is calculated based on the scheduled load at *Stage 1*, i.e. $P^{S1,L}_{t\mu}$, and the realized demand-side contributions $LR^{S2,D}_{t\omega\mu}$ and $LR^{S2,U}_{t\omega\mu}$:

$$P^{S2,L}_{t\omega\mu} = \gamma^{L}_{t\omega\mu}P^{S1,L}_{t\mu} - LR^{S2,D}_{t\omega\mu} + LR^{S2,U}_{t\omega\mu} \quad (36)$$

$$0 \leq LR^{S2,D}_{t\omega\mu} \leq LR^{S1,D}_{t\mu} \quad (37)$$

$$0 \leq LR^{S2,U}_{t\omega\mu} \leq LR^{S1,U}_{t\mu} \quad (38)$$

In (36), the coefficient $\gamma^{L}_{t\omega\mu}$ is the load realization factor which models the load uncertainties in real-time operation. For a given deterministic load, $\gamma^{L}_{t\omega\mu}$ is 1; however, for a probabilistic load, $\gamma^{L}_{t\omega\mu}$ varies based on the associated PDF. Finally, (37) and (38) determine the upper and lower boundaries for the deployment of demand-side reserves.

2.5 Constraints of Stage 3

This stage deals with the islanding and resynchronization events of an MG from the islanded NMGs. To offer more details, *Stage 2* studies the real-time operation of NMGs along with its islanding and resynchronization from the upstream network; however, *Stage 3* covers the islanding and resynchronization events for the MGs within an islanded NMGs. Similar to *Stage 1* and *Stage 2*, power balance is the main constraint:

$$P^{S3,Net}_{t\varphi\mu} + P^{S3,DG}_{t\varphi\mu} + P^{S3,Wind}_{t\varphi\mu} - P^{S3,Bat+}_{t\varphi\mu} + P^{S3,Bat-}_{t\varphi\mu} - P^{S3,L}_{t\varphi\mu} + P^{Shed}_{t\varphi\mu} = 0 \quad (39)$$

In (39), the power transaction of each MG with the rest of the islanded NMGs $P^{S3,Net}_{t\varphi\mu}$ is calculated as:

$$P^{S3,Net}_{t\varphi\mu} = \psi_{t\varphi\mu}P^{S2,Net}_{t\omega\mu} \quad (40)$$

$$\psi_{t\varphi\mu} = \begin{cases} 0 & T^{Island}_{\varphi\mu} \leq t \leq T^{Rsynch}_{\varphi\mu} \\ 1 & \text{Otherwise} \end{cases} \quad (41)$$

where $T^{Island}_{\varphi\mu}$, $T^{Rsynch}_{\varphi\mu}$ are islanding and resynchronization time for each MG. In case of islanding, i.e. $\psi_{t\varphi\mu} = 0$, the power transaction between the MG and the rest of the

NMGs $P^{S3,Net}_{t\varphi\mu}$ would be zero which might end in violations in (39). During such situation, the model can take advantages of storage system, use local DG at MG level, and finally shed some loads. This approach can be adopted until the resynchronization time and then, proper decisions after resynchronization can be realized. Such decisions should be made subject to technical constraints of the DG, storage system, and load availability within the MG:

$$\alpha^{S3,DG}_{t\varphi\mu} P^{DG,\min}_{\mu} \le P^{S3,DG}_{t\varphi\mu} \le \alpha^{S3,DG}_{t\varphi\mu} P^{DG,\max}_{\mu} \tag{42}$$

$$\begin{cases} u^{S3,SU}_{t\varphi\mu} \ge \alpha^{S3,DG}_{t\varphi\mu} - \alpha^{S3,DG}_{(t-1)\varphi\mu} \\ u^{S3,SU}_{t\varphi\mu} \ge 0 \\ u^{S3,SU}_{t\varphi\mu} \le 1 - u^{S2,SU}_{t\omega\mu} \end{cases} \tag{43}$$

$$0 \le P^{S3,Bat+}_{t\varphi\mu} \le \alpha^{S3,Bat}_{t\varphi\mu} P^{Bat+,\max}_{\mu} \tag{44}$$

$$0 \le P^{S3,Bat-}_{t\varphi\mu} \le \eta^{Bat}_{\mu}\left(1 - \alpha^{S3,Bat}_{t\varphi\mu}\right) P^{Bat-,\max}_{\mu} \tag{45}$$

$$SoC^{S3,Bat}_{t\varphi\mu} = SoC^{S3,Bat}_{(t-1)\varphi\mu} + \frac{\eta^{Bat}_{\mu}\Delta t}{E^{Bat,\max}_{\mu}}\left(P^{S3,Bat+}_{(t-1)\varphi\mu} - \left(\eta^{Bat}_{\mu}\right)^{-2} P^{S3,Bat-}_{(t-1)\varphi\mu}\right) \tag{46}$$

$$SoC^{Bat,\min}_{\mu} \le SoC^{S3,Bat}_{t\varphi\mu} \le SoC^{Bat,\max}_{\mu} \tag{47}$$

Constraint (42) represents the permissible upper and lower limits for conventional DG. Here, (43) determines the operation status of DG implying that if the DG has already started at *Stage 2*, i.e., $u^{S2,SU}_{t\omega\mu} = 0$, associated start-up cost should not be reflected in the objective function. In addition, the charging and discharging level of the storage unit as well as associated SoC should remain within a permissible limit which is modeled by (44)-(45) and (46)-(47), respectively.

In case of any inadequacy in power generation, load shedding is inevitable which should not exceed the MG load:

$$0 \le P^{Shed}_{t\varphi\mu} \le P^{S3,L}_{t\varphi\mu} \tag{48}$$

where the load at this stage is equal to that of *Stage 2*:

$$P^{S3,L}_{t\varphi\mu} = P^{S2,L}_{t\omega\mu} \tag{49}$$

Once the formulation for each step is devised, the resilience-constrained scheduling of NMGs can be achieved by minimizing (1) subject to (6)-(49), which is solved monolithically. Therefore, all the decision variables including the decisions made at *Stage 1*, *Stage 2*, and *Stage 3* mutually impact each other. The main ties between different stages are as follows:

Link 1: (20) and (21) are the first link which connects the purchase decisions in *Stage 2* to the decision made at *Stage 1*.
Link 2: (36) connects the load at *Stage 2* to the load determined in *Stage 1*, i.e., (11).
Link 3: (37) and (38) provide the link between demand-side reserve deployments in *Stage 2* and the scheduled one at *Stage 1* which is also reflected in the objective function.
Link 4: (40) and (49) are the link between *Stages 2* and *3*.

To offer more details, Link 3 is discussed as an instance. At first glance, *Stage 1* might schedule zero demand-side reserve as the objective is cost minimization. Therefore, the upper and lower bound associated with the load reserve deployment in (37) and (38) would be zero, which might end in violations in (29), i.e., real-time load at *Stage 2*. To meet (29), the scheduled demand-side reserve at *Stage 1*, i.e., (13) and (14), should be revisited. In other words, the constraints at *Stage 2* steer the decision in *Stage 1*. The similar discussion is valid for the other links implying the mutual effect of stages. The tailored problem includes binary variables and linear constraints which lies within the mixed-integer linear programming model.

2.6 Scenario generation

In order to solve the proposed stochastic programming-based model, a proper suite of scenarios should be generated and fed into the model. To cover all possible events, a great number of scenarios should be generated which challenges the tractability of the problem. In this paper, the three-point estimate method [20] is used which offers limited, but representative number of points to be evaluated while covering most of plausible circumstances.

Given the arrays of random variables at *Stages 2* and *3* as (50) and (51):

$$\boldsymbol{x}^{S2} = \begin{bmatrix} \lambda^{RT,Buy} & \lambda^{RT,Sell} & \gamma^{L} & P^{Wind} & T^{Island}_{N\mu} & T^{Rsynch}_{N\mu} \end{bmatrix} = \begin{bmatrix} x_1 & x_2 & x_3 & x_4 & x_5 & x_6 \end{bmatrix} \tag{50}$$

$$\boldsymbol{y}^{S3} = \begin{bmatrix} T^{Island}_{\mu} & T^{Rsynch}_{\mu} \end{bmatrix} = \begin{bmatrix} y_1 & y_2 \end{bmatrix} \tag{51}$$

Three points are estimated for each random variable which are denoted by index k in this paper. The set of scenarios for each stage are:

$$\Omega^{S2} = \left\{\left(\bar{x}_1, \ldots, x_{l,k}, \ldots \bar{x}_6\right)\right\} \quad l = 1, 2, \ldots, 6 \quad k = 1, 2, 3 \tag{52}$$

$$\Omega^{S3} = \{(y_{1,k}, \bar{y}_2), (\bar{y}_1, y_{2,k})\} \quad k = 1, 2, 3 \tag{53}$$

where $^-$ denotes the expected value of associated random variable and:

$$\begin{cases} x_{l,k} = \bar{x}_l + \zeta_{l,k}\tilde{x}_l \\ y_{l,k} = \bar{y}_l + \zeta_{l,k}\tilde{y}_l \end{cases} \tag{54}$$

$$\zeta_{l,k} = \begin{cases} \dfrac{\upsilon_l}{2} + \sqrt{\kappa_l - \dfrac{3}{4}\upsilon_l^2} & k = 1 \\ \dfrac{\upsilon_l}{2} - \sqrt{\kappa_l - \dfrac{3}{4}\upsilon_l^2} & k = 2 \\ 0 & k = 3 \end{cases} \tag{55}$$

In (54) and (55), $(\tilde{\cdot})$, υ_l, κ_l symbolizes the standard deviation, Skewness and Kurtosis of associated random variable, respectively. Once the scenarios are attained, the probability for realization of each scenario is calculated as:

$$\pi = \begin{cases} \dfrac{(-1)^{3-k}}{\zeta_k(\zeta_1 - \zeta_2)} & k = 1, 2 \\ 1 - \dfrac{1}{\kappa - \upsilon^2} & k = 3 \end{cases} \tag{56}$$

Note that trimming the scenario numbers down is a common practice to render the stochastic programming-based problems more tractable. In other words, scenario reduction approach is essential in cases of dealing with great number of scenarios such as outputs of Monte-Carlo-based scenario generation approach. However, the point estimate method used in this paper offers limited, but representative number of scenarios. Here, the number of representative scenarios is twice of the number of uncertain parameters plus one. Note that for the proposed approach, the scenarios are considered as the input and the tailored model can be evaluated apart from the scenario generation and reeducation approach. The point estimate method is used due to the associated advantages and replacing this approach with any scenario generation and reduction approach would not affect the performance of the proposed method.

3 Simulation study

This section examines the proposed three-stage scheme on the system depicted in Fig. 2. For the simulation studies, two MGs are considered which represent NMGs. The data associated with the DG units and storage systems are reported in Tables 1 and 2, respectively. The maximum wind generation for each MG is considered 1 MW while considering 5 MW as the total load of each MG.

A statistical analysis is made on the Turkish Energy Exchange Platform (EXIST) [21] to attain realistic PDFs for market price, load profile, and wind generation. The timespan July 1-29, 2018 is considered and the calculated PDFs are depicted in Fig. 3. Finally, the probability distribution parameters for the islanding and resynchronization events are given in Table 3 [4].

By the proposed scenario generation scheme in place, the real-time value of market price, load amount, and wind

Table 1 Technical data for DG units

Unit	$P^{\max}$ (MW)	$P^{\min}$ (MW)	λ^{DG} ($/MW)	λ^{SU} ($)
DG1	3	0.21	37	55
DG2	2	0.19	37	55

Table 2 Technical data for storage units

Unit	$E^{\max}$ (MW)	$P^{+(-)\max}$ (MW)	$SoC^{\max}$
Battery1	1.5	0.5	0.90
Battery2	1.0	0.3	0.95

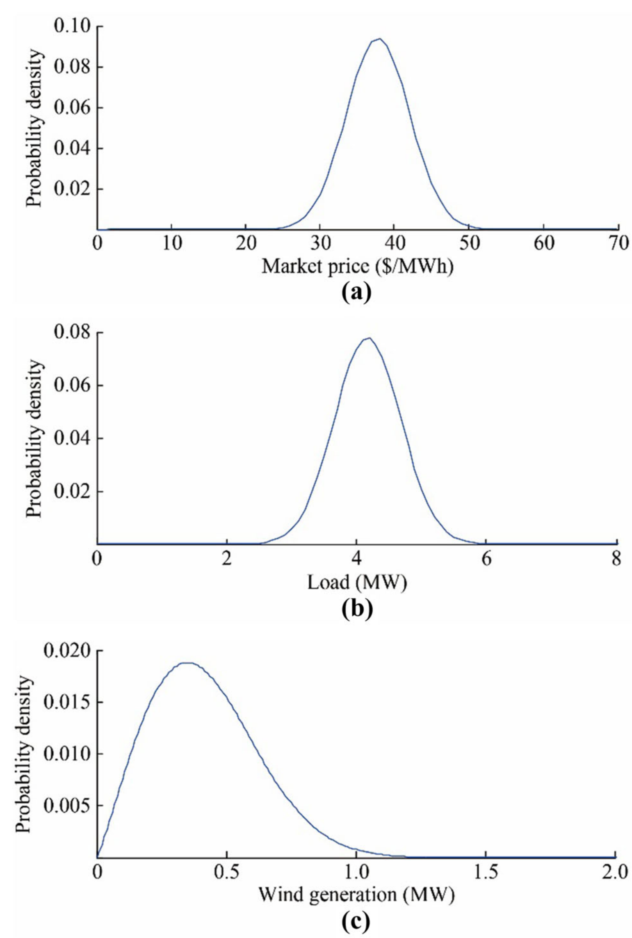

Fig. 3 Calculated PDFs for market price, load, and wind generation

Table 3 Probability distribution parameters for islanding and resynchronization

Parameter	PDF	Mean	Standard deviation	Range
$T_{N\mu}^{Island}$	Normal	15	1	[12–18]
$T_{N\mu}^{Rsynch}$	Normal	20	1	[17–23]
T_{μ}^{Island}	Normal	15	1	[13–17]
T_{μ}^{Rsynch}	Normal	18	1	[17–19]

generation corresponding with each scenario is depicted in Figs. 4, 5, and 6, respectively. Note that the same load profile and wind pattern are assumed for each MG.

In this study, the following case studies are conducted.

Case 1: The scheduling of NMGs and taking the uncertainties of market price, load amount, and wind generation into account

Case 2: Case 1 plus uncertainties pertaining to unintentional islanding of NMGs from the upstream network and resynchronization

Case 3: Case 2 plus uncertainties pertaining to unintentional islanding of the MGs from the rest NMGs and resynchronization

The corresponding cases are simulated in GAMS® IDE environment and solved with CPLEX® 12.4 using a personal computer with Intel Core^{TM} i7 CPU @3 GHz and 12 GB RAM.

Table 4 summarizes the results of simulation studies for Case 1. The total cost is \$857.75. The overall computation time associated with this case is around 0.06 s. Referring to Table 4, the EC associated with *Stage 2* and *Stage 3* is relatively lower than that of *Stage 1*. The reason is that the cost at *Stage 1* is the cost of serving total load; whereas, the EC of *Stage 2* and *Stage 3* is the cost of handling minor operational uncertainties.

Figure 7 depicts the contribution of market, DG, and wind generation in supplying the load (scenario #6). As can be seen from Fig. 7, the role of the market is dominant at

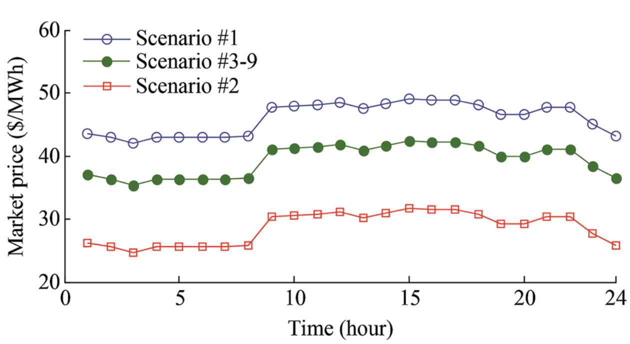

Fig. 4 Real-time market price at each scenario

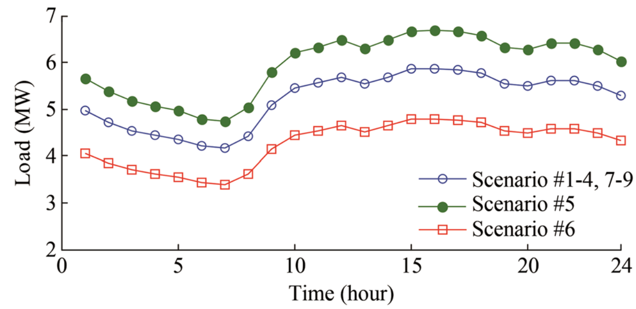

Fig. 5 Real-time load amount at each scenario

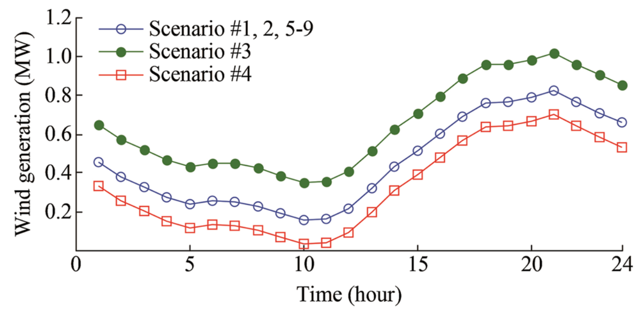

Fig. 6 Real-time wind generation at each scenario

Table 4 Result of Case 1

Time (hour)	Cost of *Stage 1* (\$)	EC of *Stage 2* and *Stage 3* (\$)
1	273.45	150.18
2	258.54	34.55
3	244.97	31.21
4	248.55	27.63
5	246.20	25.74
6	236.23	25.87
7	233.33	25.74
8	252.39	25.40
9	334.51	27.09
10	368.67	31.26
11	376.85	31.60
12	378.74	29.05
13	351.74	33.97
14	359.36	40.49
15	370.92	45.38
16	362.71	50.30
17	353.84	55.26
18	346.93	64.99
19	314.83	67.86
20	307.84	70.88
21	320.04	75.42
22	329.91	67.51
23	298.12	68.77
24	248.03	48.87

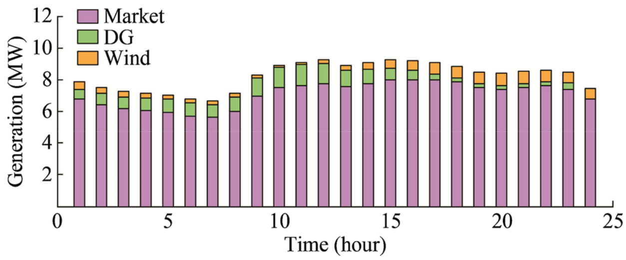

Fig. 7 Share of market, DG, and wind generation in supplying the load (Case 1, scenario #6)

each time slot and a great share of load is supplied by the market. In spite of being a low-cost solution, such scheduling is not resilient since considerable amount of load should be shed in case of unintentional islanding. For instance, around 7.8 MW load shedding at each hour (62 MWh) is inevitable if an unintentional islanding happens at the time slot between 14 and 21.

Table 5 reports the results of simulation studies for Case 2, where the uncertainties pertaining to unintentional islanding of NMGs from the upstream network are also considered. The total cost is $9938.55. In addition, the contribution of market, DG, and wind generation in supplying the load is depicted in Fig. 8 (scenario #6).

As can be seen, the share of market is reduced to minimize the load shedding in case of unintentional islanding. The total cost is slightly increased in comparison to Case 1 which is the cost of resilience. Comparing Tables 4 and 5, we can find that the EC at the time slot between 14 and 19 is increased, which is the most probable period for islanding is shown in Table 3. If an unintentional islanding happens at the time slot between 14 and 21, the amount of load shedding would be 22.43 MWh which is much less than Case 1. The overall computation time associated with Case 2 is around 0.06 s.

The simulation results for Case 3 are summarized in Table 6 where the islanding of individual MGs from the rest of NMGs is also taken into account. The total cost is $11934.4. According to (40), the islanding is envisioned for all MGs within the NMGs, which is realized based on the designed scenarios. As the simulated NMGs include two MGs, the islanding of one MG from NMGs results in the islanding of the other MG. The conducted study takes the islanding of both MGs into the account.

Referring to Table 6, the cost increment comparing to Table 5 is occurred at the time slot between 15 and 18. The reason is that referring to Table 3, the islanding of an MG from the rest of NMGs is most likely to happen in this period. In this case, around 14 MWh load shedding might happen in case of islanding at the time slot between 14 and 21. Figure 9 depicts the total cost and load shedding amount versus the envisioned stages of islanding.

Table 5 Result of Case 2

Time (hour)	Cost of *Stage 1* ($)	EC of *Stage 2* and *Stage 3* ($)
1	273.45	150.18
2	258.54	34.55
3	244.97	31.21
4	248.55	27.63
5	246.20	25.74
6	236.23	25.87
7	233.33	25.74
8	252.39	25.40
9	334.51	27.09
10	368.67	31.26
11	376.85	31.60
12	378.74	29.05
13	351.74	33.97
14	359.36	40.49
15	370.92	377.51
16	362.71	361.64
17	353.84	353.00
18	336.49	333.20
19	308.24	297.50
20	303.43	72.78
21	317.28	77.32
22	322.21	69.48
23	298.12	62.12
24	248.03	48.87

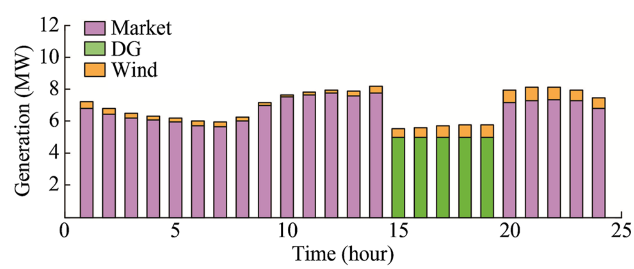

Fig. 8 Share of market, DG, and wind generation in supplying the load (Case 2, scenario #6)

As can be seen from Fig. 9, by increasing the stages of islanding, the total cost increases; on the contrary, the amount of load shedding decreases. In other words, the resilience of distribution system enhances as we increase the number of distributed elements. The overall computation time associated with this case is also around 0.06 s.

Table 6 Result of Case 3

Time (hour)	Cost of *Stage 1* ($)	EC of *Stage 2* and *Stage 3* ($)
1	429.35	59.82
2	286.14	100.08
3	268.33	35.49
4	268.11	31.40
5	263.62	29.11
6	254.35	29.36
7	251.45	29.23
8	269.17	28.68
9	350.13	30.86
10	379.41	32.13
11	387.62	32.48
12	397.17	33.62
13	377.91	40.24
14	395.14	49.28
15	631.77	577.01
16	631.12	560.29
17	412.11	367.63
18	399.63	348.67
19	369.72	311.68
20	375.32	73.91
21	391.03	78.44
22	400.89	73.81
23	373.54	66.42
24	299.73	52.00

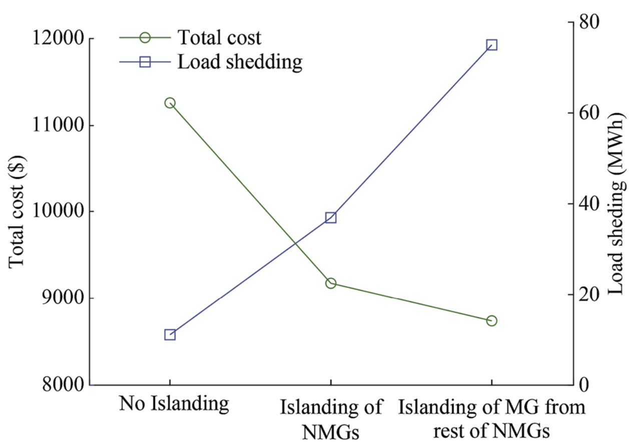

Fig. 9 Cost and load shedding amount versus envisioned stages of islanding

4 Conclusion

In this paper, a new model for resiliency-oriented scheduling of NMGs is presented. A three-stage stochastic programming-based approach is devised in which uncertainties pertaining to the renewable generation, market price, power consumption of loads, unintentional islanding of NMGs from the upstream network, and unintentional islanding of an MG from the rest of NMGs are embedded. The effectiveness of the proposed scheme is verified by several simulation studies which concluded that: ① damaging impacts of electricity interruptions can be mitigated by effectively exploiting the NMG capabilities; ② prognosis of the plausible uncertainties and considering of associated effects in the scheduling stage can enhance the security and economy of power systems; ③ the resilience of power system improves by increasing the number of distributed elements such as those offered by NMGs.

Acknowledgment This paper presents the scientific results of the project "Intelligent system for trading on wholesale electricity market" (SMARTRADE), co-financed by the European Regional Development Fund (ERDF), through the Competitiveness Operational Program (COP) 2014-2020, priority axis 1 – Research, technological development and innovation (RD&I) to support economic competitiveness and business development, Action 1.1.4 - Attracting high-level personnel from abroad in order to enhance the RD capacity, contract ID P_37_418, no. 62/05.09.2016, beneficiary The Bucharest University of Economic Studies. In addition, this paper is supported by TÜBİTAK TEYDEB program (No. 7170150).

References

[1] Li Z, Shahidehpour M, Aminifar F et al (2017) Networked microgrids for enhancing the power system resilience. Proc IEEE 105(7):1289–1310

[2] Wang X, Shahidehpour M, Jiang C et al (2018) Resilience enhancement strategies for power distribution network coupled with urban transportation system. IEEE Trans Smart Grid. https://doi.org/10.1109/tsg.2018.2848970

[3] Wang Y, Huang LP, Shahidehpour M et al (2018) Resilience-constrained hourly unit commitment in electricity grids. IEEE Trans Power Syst 33(5):5604–5614

[4] Wang Y, Chen C, Wang J et al (2016) Research on resilience of power systems under natural disasters—a review. IEEE Trans Power Syst 31(2):1604–1613

[5] Panteli M, Mancarella P, Trakas DN et al (2017) Metrics and quantification of operational and infrastructure resilience in power systems. IEEE Trans Power Syst 32(6):4732–4742

[6] Ouyang M, Duenas-Osorio L (2014) Multi-dimensional hurricane resilience assessment of electric power systems. Struct Saf 48:15–24

[7] Khodaei A (2015) Provisional microgrids. IEEE Trans Smart Grid 6(3):1107–1115

[8] Ton DT, Wang WP (2015) A more resilient grid: the US department of energy joins with stakeholders in an R&D plan. IEEE Power Energy Mag 13(3):26–34

[9] Resende F, Gil NJ, Lopes JP (2011) Service restoration on distribution systems using multi-microgrids. Eur Trans Electr Power 21(2):1327–1342
[10] Khodaei A (2014) Resiliency-oriented microgrid optimal scheduling. IEEE Trans Smart Grid 5(4):1584–1591
[11] Tsikalakis AG, Hatziargyriou ND (2011) Operation of microgrids with demand side bidding and continuity of supply for critical loads. Eur Trans Electr Power 21(2):1238–1254
[12] Gouveia C, Moreira J, Moreira C et al (2013) Coordinating storage and demand response for microgrid emergency operation. IEEE Trans Smart Grid 4(4):1898–1908
[13] Trakas DN, Hatziargyriou ND (2018) Optimal distribution system operation for enhancing resilience against wildfires. IEEE Trans Power Syst 33(2):2260–2271
[14] Gholami A, Shekari T, Aminifar F et al (2016) Microgrid scheduling with uncertainty: The quest for resilience. IEEE Trans Smart Grid 7(6):2849–2858
[15] Wang C, Hou Y, Qiu F et al (2017) Resilience enhancement with sequentially proactive operation strategies. IEEE Trans Power Syst 32(4):2847–2857
[16] Amirioun M, Aminifar F, Lesani H (2018) Towards proactive scheduling of microgrids against extreme floods. IEEE Trans Smart Grid 9(4):3900–3902
[17] Amirioun M, Aminifar F, Lesani H (2018) Resilience-oriented proactive management of microgrids against windstorms. IEEE Trans Power Syst 33(4):4275–4284
[18] Conejo AJ, Carrión M, Morales JM (2010) Decision making under uncertainty in electricity markets. Springer, Berlin
[19] Teimourzadeh S, Mohammadi-Ivatloo B (2014) Probabilistic power flow module for powerfactory digsilent. Springer, Cham
[20] Morales JM, Perez-Ruiz J (2007) Point estimate schemes to solve the probabilistic power flow. IEEE Trans Power Syst 22(4):1594–1601
[21] https://seffaflik.epias.com.tr/transparency/index.xhtml. Accessed 3 November 2018

Saeed TEIMOURZADEH received the Ph.D. degree in power electrical engineering from School of Electrical and Computer Engineering, University of Tehran, Tehran, Iran, in 2018. From 2016 to 2017, he was a Research Associate with the Electrical and Computer Engineering Department at the Illinois Institute of Technology (IIT), Chicago, USA. He is currently a deputy director (projects) with EPRA Electric Energy Co., Ankara, Turkey. He served as the editor of the Journal of Modern Power Systems and Clean Energy (MPCE) and received the 2018 Excellence in Reviewing award from MPCE Journal. His research interests include microgrid protection, control and stability, and smart grid initiatives.

Osman Bulent TOR received his B.S., M.S. and Ph.D. degrees from Middle East Technical University (METU), Turkey, in 1998, 2001 and 2008, respectively. He is working as a managing partner and director at EPRA Electric Energy Co., Ankara, Turkey.

Mahmut Erkut CEBECI received his B.S. and M.S. degrees from Middle East Technical University (METU), Ankara, Turkey, in 2005 and 2008, respectively. He is working as a managing partner and director at EPRA Electric Energy Co., Ankara, Turkey.

Adela BARA graduated from the Faculty of Economic Cybernetics in 2002, holds a Ph.D. diploma in Economics from 2007. She is professor at the Economic Informatics Department at the Faculty of Cybernetics, Statistics and Economic Informatics from The Bucharest University of Economic Studies, Romania and coordinated three R&D projects. Her research interests are focused on in data science, analytics, databases, big data, data mining, power systems, authoring more than 70 papers in international journals and conferences.

Simona Vasilica OPREA received the MSc degree through the Infrastructure Management Program from Yokohama National University, Japan, in 2007, the first Ph.D. degree in Power System Engineering from the Bucharest Polytechnic University in 2009, and the second Ph.D. degree in Economic Informatics from the Bucharest University of Economic Studies, Romania in 2017. She is currently an Assistant Professor with the Faculty of Cybernetics, Statistics, and Economic Informatics with the Bucharest Academy of Economic Studies, involved in several research projects.